Pergamon

Int. J. Solids Structures Vol. 31, No. 5, pp. 657–667, 1994
Elsevier Science Ltd
Printed in Great Britain
0020–7683/94 \$6.00 + .00

STATIC AND DYNAMIC ANALYSIS OF ARBITRARY QUADRILATERAL FLEXURAL PLATES BY B_3-SPLINE FUNCTIONS

GANG WANG and CHENG-TZU THOMAS HSU
Department of Civil and Environmental Engineering, New Jersey Institute of Technology, Newark, New Jersey 07102, U.S.A.

(*Received* 3 *February* 1993; *in revised form* 2 *August* 1993)

Abstract—This paper presents static and free vibration analysis of arbitrary quadrilateral flexural plates by B_3-spline functions. An actual arbitrary quadrilateral thin flat plate is mapped onto a square basic plate and a superelement is constructed for the whole plate. The present numerical analysis is based on a spline net with finite spline points on the square basic plate. Combination of B_3-spline functions gives an easy way to satisfy various boundary conditions. The displacement function constructed by B_3-spline functions in two directions has been formed to possess more flexibility to model the deflection shape efficiently. The main features of the present method are: minimal input preparation, easier programming and higher accuracy achieved by a system with fewer degrees of freedom. Compared with analytical solutions and other numerical methods, the method proposed yields excellent results for the test cases considered.

INTRODUCTION

The spline functions are important tools in the analysis of plates and shells. They are computationally efficient, and flexible to model different geometrical shape and boundary conditions. In the past decade, some researchers have used the spline functions in numerical structural analysis. The conventional functions, such as the polynomial functions, the trigonometric functions, etc. are replaced by the spline functions for interpolation of displacement. Qin (1982) presented the spline finite point method for the analysis of linear elastic straight beams and flat plates and he displayed excellent analytical results on the rectangular plates. This method has been extended to study a variety of structures which include static, dynamic, and stability problems (Qin, 1985). The solution of plate analysis by the spline finite point method is usually restricted to plate geometry with rectangular shape. The conventional finite strip method was modified by Cheung *et al.* (1982) who then developed the spline finite strip method. In the spline finite strip method, the trigonometric functions for the interpolation of displacement used in the conventional finite strip method were replaced by the B_3-spline functions in the longitudinal direction. Several investigators have successfully solved various plate problems recently using the spline finite strip method (Li *et al.*, 1986; Tham *et al.*, 1986). Various other authors have developed different spline finite elements for beams, plates and shells, respectively. The element efficiency due to the choice of the spline functions has been demonstrated in their studies. In the spline finite elements for beams and plates presented by Leung and Au (1990), the physical coordinates were introduced into the formulation, which made the assembly of elements possible. These elements could only be used for plates with rectangular shape, although they were able to deal with the various boundary conditions. More computation had to be carried out due to the matrix transformation between the spline coordinates and the physical coordinates in this approach. Fan and Luah (1992) employed a set of B-spline shape functions for the displacement interpolation to develop a new spline finite element for plate bending. The element had nine nodes, in the shape of an arbitrary quadrilateral with biquadratic Lagrangian shape functions for geometric interpolation. It has been shown in their research that the use of B-spline functions generally yields an excellent result in two-dimensional structural analysis. However, a lot of input data due to the mesh generation has to be prepared carefully. Also, the exclusion of the twisting curvatures at corner nodes impairs the accuracy of the element in their method.

SAS 31:5-F

In the present paper, the efficient B_3-spline functions are employed in two directions for the interpolation of displacement to study the static and dynamic behavior of thin flat plates with arbitrary quadrilateral shapes. Compared with other numerical methods of using the spline functions for plate analysis, the present method may be found new in the following:

1. In the present method, the entire deformed shape of a plate can be described with only one displacement function constructed by a series of B_3-spline functions. The mesh generation and large computer-memory space, drawbacks of the discretization methods, are no longer needed because only one single superelement is used in the whole process.
2. With the help of proper geometrical mapping, the present method can be used to analyse arbitrary quadrilateral plates. The plate geometries considered in the spline finite point method proposed by Qin (1982, 1985) and in the spline finite elements developed by Leung and Au (1990) were restricted to rectangular shape.
3. More flexibility of the displacement field in the present method can be obtained by applying B_3-spline functions in two directions. The displacement functions in the spline finite point method and in the spline finite strip method were constructed by B-spline functions in one direction and nonspline functions in another direction.
4. Due to the appropriate combination of B_3-spline functions in the displacement field, the present method avoids the inverse computation resulting from the matrix transformation which occurs in the spline finite element method.
5. The necessary degrees of freedom to maintain the completeness of the displacement function, including the twisting curvatures at corner nodes, are all retained in the present method. In the spline finite elements developed by Fan and Luah (1992), the unavoidable approximate treatment of the twisting curvatures at corner nodes impairs the accuracy of the solutions.

Accuracy, efficiency, and simplicity of the present method will be demonstrated in the following description and numerical examples.

GEOMETRICAL MAPPING

An arbitrary quadrilateral plate in the x–y plane is shown in Fig. 1(a). It can be mapped into a 2×2 square region in the r–s plane [Fig. 1(b)], if the Cartesian coordinates x and y within the plate are defined by:

$$x = \sum_{i=1}^{4} N_i x_i \quad y = \sum_{i=1}^{4} N_i y_i, \tag{1}$$

where x_i and y_i are the coordinates of node i in x–y plane. The shape functions N_i for mapping can be expressed as follows:

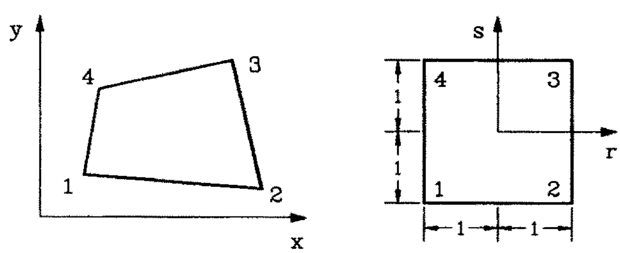

(a) Actual plate (b) Basic plate

Fig. 1. Geometrical mapping.

$$N_i = (1+r_0)(1+s_0)/4 \quad (i = 1,2,3,4), \tag{2}$$

where $r_0 = r_i r$ and $s_0 = s_i s$; r_i and s_i are the coordinates of node i in r–s plane. For any higher order complex shape, the analysis procedure is straightforward so long as the appropriate mapping functions are selected.

By the chain rule of differentiation, the first and second derivatives of displacement w for the two coordinate systems are related as:

$$\begin{Bmatrix} \dfrac{\partial w}{\partial x} \\ \dfrac{\partial w}{\partial y} \end{Bmatrix} = \mathbf{J}^{-1} \begin{Bmatrix} \dfrac{\partial w}{\partial r} \\ \dfrac{\partial w}{\partial s} \end{Bmatrix}, \tag{3}$$

$$\chi = -\begin{Bmatrix} \dfrac{\partial^2 w}{\partial x^2} \\ \dfrac{\partial^2 w}{\partial y^2} \\ 2\dfrac{\partial^2 w}{\partial x\,\partial y} \end{Bmatrix} = \mathbf{J2}^{-1}\left[\mathbf{J1J}^{-1} \begin{Bmatrix} \dfrac{\partial w}{\partial r} \\ \dfrac{\partial w}{\partial s} \end{Bmatrix} - \begin{Bmatrix} \dfrac{\partial^2 w}{\partial r^2} \\ \dfrac{\partial^2 w}{\partial s^2} \\ \dfrac{\partial^2 w}{\partial r\,\partial s} \end{Bmatrix} \right], \tag{4}$$

where

$$\mathbf{J} = \begin{bmatrix} \dfrac{\partial x}{\partial r} & \dfrac{\partial y}{\partial r} \\ \dfrac{\partial x}{\partial s} & \dfrac{\partial y}{\partial s} \end{bmatrix} \qquad \mathbf{J1} = \begin{bmatrix} \dfrac{\partial^2 x}{\partial r^2} & \dfrac{\partial^2 y}{\partial r^2} \\ \dfrac{\partial^2 x}{\partial s^2} & \dfrac{\partial^2 y}{\partial s^2} \\ \dfrac{\partial^2 x}{\partial r\,\partial s} & \dfrac{\partial^2 y}{\partial r\,\partial s} \end{bmatrix},$$

$$\mathbf{J2} = \begin{bmatrix} \left(\dfrac{\partial x}{\partial r}\right)^2 & \left(\dfrac{\partial y}{\partial r}\right)^2 & \dfrac{\partial x}{\partial r}\dfrac{\partial y}{\partial r} \\ \left(\dfrac{\partial x}{\partial s}\right)^2 & \left(\dfrac{\partial y}{\partial s}\right)^2 & \dfrac{\partial x}{\partial s}\dfrac{\partial y}{\partial s} \\ \dfrac{\partial x}{\partial r}\dfrac{\partial x}{\partial s} & \dfrac{\partial y}{\partial r}\dfrac{\partial y}{\partial s} & \dfrac{1}{2}\left(\dfrac{\partial x}{\partial r}\dfrac{\partial y}{\partial s} + \dfrac{\partial x}{\partial s}\dfrac{\partial y}{\partial r}\right) \end{bmatrix},$$

and where J and χ are the Jacobian matrix and the plate curvature matrix respectively.

These above relations will be used in the later derivation of the present numerical analysis.

DISPLACEMENT FUNCTION

A basic plate of dimension 2×2 as shown in Fig. 1(b) is divided in r and s directions with N and M equal sections, respectively, i.e.

$$-1 = r_0 < r_1 < r_2 \cdots < r_n = 1,$$

$$-1 = s_0 < s_1 < s_2 < \cdots < s_m = 1,$$

where

$$r_i = r_0 + ih_r \quad h_r = 2/N,$$
$$s_j = s_0 + jh_s \quad h_s = 2/M.$$

By doing so, a mesh with $(N+1)\times(M+1)$ spline finite points is spread on the plate.

The displacement function of the mid-surface is based on these spline finite points and may be expressed as:

$$w = \sum_{j=-1}^{M+1} \sum_{i=-1}^{N+1} c_{ij}\phi_i(r)\psi_j(s) = \mathbf{QC} \tag{5}$$

where

$$\mathbf{Q} = \mathbf{\Psi} \otimes \mathbf{\Phi} = [\psi_j \mathbf{\Phi}]$$
$$\mathbf{\Phi} = [\phi_{-1} \quad \phi_0 \quad \phi_1 \ldots \phi_{N+1}]$$
$$\mathbf{\Psi} = [\psi_{-1} \quad \psi_0 \quad \psi_1 \ldots \psi_{M+1}]$$
$$\mathbf{C} = [c_{-1}^T \quad c_0^T \quad c_1^T \ldots c_{M+1}^T]^T$$
$$\mathbf{c}_j^T = [c_{-1j} \quad c_{0j} \quad c_{1j} \ldots c_{(N+1)j}],$$

and $\mathbf{\Psi} \otimes \mathbf{\Phi}$ is the Kronecker product of the row matrices $\mathbf{\Psi}$ and $\mathbf{\Phi}$; $\mathbf{C}$ is the generalized spline coordinate column matrix with dimension $(N+3)(M+3)$.

B_3-spline function can be found as:

$$\varphi_3(z) = \frac{1}{6}\begin{cases} (z+2)^2, & z \in [-2,-1] \\ (z+2)^3 - 4(z+1)^3, & z \in [-1,0] \\ (2-z)^3 - 4(1-z)^3, & z \in (0,1] \\ (2-z)^3, & z \in [1,2] \\ 0, & |z| \geqslant 2, \end{cases} \tag{6}$$

and is used to construct ϕ_i and ψ_j as shown in the following:

$$\begin{aligned}
\phi_{-1} &= 1.5\varphi_3\left(\frac{r+1}{h_r}\right), \\
\phi_0 &= 0.5h_r\varphi_3\left(\frac{r+1}{h_r}\right) - 2h_r\varphi_3\left(\frac{r+1}{h_r}+1\right), \\
\phi_1 &= \varphi_3\left(\frac{r+1}{h_r}-1\right) - 0.5\varphi_3\left(\frac{r+1}{h_r}\right) + \varphi_3\left(\frac{r+1}{h_r}+1\right), \\
\phi_2 &= \varphi_3\left(\frac{r+1}{h_r}-2\right), \\
&\vdots \\
\phi_{N-2} &= \varphi_3\left(\frac{r+1}{h_r}-N+2\right), \\
\phi_{N-1} &= \varphi_3\left(\frac{r+1}{h_r}-N+1\right) - 0.5\varphi_3\left(\frac{r+1}{h_r}-N\right) + \varphi_3\left(\frac{r+1}{h_r}-N-1\right), \\
\phi_N &= 1.5\varphi_3\left(\frac{r+1}{h_r}-N\right), \\
\phi_{N+1} &= 2h_r\varphi_3\left(\frac{r+1}{h_r}-N-1\right) - 0.5h_r\varphi_3\left(\frac{r+1}{h_r}-N\right).
\end{aligned} \tag{7}$$

Replacing r with s, h_r with h_s and N with M, one can have the similar expressions for ψ_j.

It is obvious from the above expressions that:

$$\phi_i(-1) = \psi_j(-1) = 0 \quad (i, j \neq -1), \qquad \phi_{-1}(-1) = \psi_{-1}(-1) = 1$$
$$\phi_i'(-1) = \psi_j'(-1) = 0 \quad (i, j \neq 0), \qquad \phi_0'(-1) = \psi_0'(-1) = 1$$
$$\phi_i(1) = \psi_j(1) = 0 \quad (i \neq N, j \neq M), \qquad \phi_N(1) = \psi_M(1) = 1$$
$$\phi_i'(1) = \psi_j'(1) = 0 \quad (i \neq N+1, j \neq M+1), \qquad \phi_{N+1}'(1) = \psi_{M+1}'(1) = 1$$

where ϕ_i' and ψ_j' represent first derivatives of ϕ_i and ψ_j.

Therefore, the treatment of the boundary conditions is easy due to the ingeniously combined displacement function. For example, eliminating ϕ_{-1} term represents a simply supported side between node 1 and 4 [Fig. 1(b)], and eliminating both ϕ_{-1} and ϕ_0 terms makes this side fixed.

FORMULATION OF PRESENT NUMERICAL ANALYSIS

The total potential energy of a Kirchhoff's bending plate can be expressed as:

$$\Pi = \frac{1}{2}\int_{-1}^{1}\int_{-1}^{1} (\chi^T \mathbf{D} \chi - 2qw)|\mathbf{J}|\, \mathrm{d}r\, \mathrm{d}s = \tfrac{1}{2}\mathbf{C}^T\mathbf{G}\mathbf{C} - \mathbf{C}^T\mathbf{f}. \tag{8}$$

Using the principle of minimum total potential energy, one obtains:

$$\mathbf{G}\mathbf{C} = \mathbf{f} \tag{9}$$

where $\mathbf{G}$ is the stiffness matrix:

$$\mathbf{G} = \int_{-1}^{1}\int_{-1}^{1} \mathbf{B}^T\mathbf{D}\mathbf{B}|\mathbf{J}|\, \mathrm{d}r\, \mathrm{d}s,$$

$$\mathbf{B} = \mathbf{J2}^{-1}\left(\mathbf{J1}\mathbf{J}^{-1}\begin{Bmatrix}\mathbf{\Psi}\otimes\mathbf{\Phi}' \\ \mathbf{\Psi}'\otimes\mathbf{\Phi}\end{Bmatrix} - \begin{Bmatrix}\mathbf{\Psi}\otimes\mathbf{\Phi}'' \\ \mathbf{\Psi}''\otimes\mathbf{\Phi} \\ \mathbf{\Psi}'\otimes\mathbf{\Phi}'\end{Bmatrix}\right). \tag{10}$$

For a plate of isotropic material, the rigiditiy matrix is:

$$\mathbf{D} = \frac{Et^3}{12(1-\mu^2)}\begin{bmatrix}1 & \mu & 0 \\ \mu & 1 & 0 \\ 0 & 0 & (1-\mu)/2\end{bmatrix},$$

where E = Young's modulus; μ = Poisson's ratio; t = thickness of the plate.

The load matrix has the form:

$$\mathbf{f} = \int_{-1}^{1}\int_{-1}^{1} \mathbf{Q}^T q|\mathbf{J}|\, \mathrm{d}r\, \mathrm{d}s, \tag{11}$$

where q = the intensity of applied load.

The functional of a thin plate for free vibration is:

$$\Pi = \frac{\pi}{2\omega}\int_{-1}^{1}\int_{-1}^{1} (\chi^T\mathbf{D}\chi - \omega^2\rho t w^2)|\mathbf{J}|\, \mathrm{d}r\, \mathrm{d}s = \frac{\pi}{2\omega}\mathbf{C}^T(\mathbf{G} - \omega^2\mathbf{M})\mathbf{C}. \tag{12}$$

According to the Hamilton's principle, one has:

$$(\mathbf{G}-\omega^2\mathbf{M})\mathbf{C} = 0, \tag{13}$$

where ω = the natural circular frequency.

The mass matrix:

$$\mathbf{M} = \int_{-1}^{1}\int_{-1}^{1} \rho t \mathbf{Q}^T\mathbf{Q}|\mathbf{J}|\,\mathrm{d}r\,\mathrm{d}s, \tag{14}$$

where ρ = the material mass density.

The integral functions of the stiffness, mass and load matrices are quite complicated so that they have to be evaluated numerically. Simpson's integration formulation is applied in the present method. The values of functions ϕ_i and ψ_j and their first and second derivatives on the spline finite points, which are needed in numerical integration and computation of displacements, rotations, and moments, are convenient to obtain.

NUMERICAL EXAMPLES

Four plate examples with various shapes and boundary conditions are selected herein to demonstrate the efficiency and applicability of the present method. Excellent performance of the present method for this type of plate problems is achieved by comparing the results with analytical solutions and those of other numerical methods, such as the finite element method (FEM) and the spline finite strip method (SFSM). Some common symbols used in the Tables of results are defined as follows: q = the intensity of uniformly distributed load on the entire plate; P = the concentrated load at midpoint of the plate; $D = Et^3/[12(1-\mu^2)]$; and Poisson's ratio $\mu = 0.3$ for all test cases in this paper.

Example 1: bending of square plate

The investigation of square plates is fundamental in the analysis of plate problems. The results of a square plate using different methods are readily available in literature and the general characteristics of using different methods may be shown by comparisons of the obtained results. Both simply supported and clamped square plates under uniformly distributed and concentrated loads are discussed in this paper. Only a quarter of the plate is considered due to dual symmetry.

Table 1 gives the central deflections of square plates obtained by the present method as well as by FEM with a basic type of element—four—node nonconforming C^1 element with 12 degrees of freedom. Computed results from both the present method and the spline finite element method (SFEM) for a simply supported square plate under uniformly

Table 1. Comparison of central deflections of simply supported and clamped square plates under uniformly distributed and central concentrated loads

Number	Clamped plate				Simply supported plate			
of	Uniform load[a]		Point load[b]		Uniform load[a]		Point load[b]	
nodes	FEM	Present	FEM	Present[b]	FEM	Present	FEM	Present
9	0.140	0.1260	0.613	0.5419	0.394	0.4064	1.23	1.143
25	0.130	0.1265	0.580	0.5567	0.403	0.4062	1.18	1.156
49	0.128	0.1265	0.571	0.5592	0.405	0.4062	1.17	1.158
81	0.127	0.1265	0.567	0.5601	0.406	0.4062	1.16	1.159
Exact	0.1265		0.560		0.4062		1.16	

[a] Multiplier = $10^{-2}qa^4/D$, [b] multiplier = $10^{-2}\,Pa^2/D$.

Table 2. Comparison of central deflection and bending moments of simply supported square plate under uniformly distributed load

Number of nodes	Central deflection[a] SFEM	Present	Bending moment[c] at center SFEM	Present	Twisting moment[c] at corner SFEM	Present
9	0.41189	0.40640	—	0.4867	—	0.3243
25	0.40675	0.40624	0.4911	0.4814	0.3554	0.3247
81	0.40627	0.40624	0.4824	0.4795	0.3390	0.3248
169	0.40642	0.40624	0.4804	0.4789	0.3330	0.3248
Exact	0.40624		0.4789		0.3248	

[a]Multiplier = $10^{-2}qa^4/D$, [c]multiplier = $10^{-1}qa^2$.

distributed load are shown in Table 2. Nine-node C^1 element in SFEM here has 21 degrees of freedom and has shown advantages over its counterparts in FEM through research carried out by Fan and Luah (1992). It should be noted, before a detailed observation on the compared results in Tables 1 and 2, that total number of unknowns without imposition of nodal restraints for FEM, SFEM and the present method are $3NM+3(N+M)+3$, $2NM+2.5(N+M)+3$ and $NM+3(N+M)+9$, respectively, under the same mesh $N \times M$ or the same number of nodes $(N+1)(M+1)$. With the imposition of nodal restraints, different methods may reduce a few and nearly the same number of unknowns for various boundary conditions. This indicates that the sequence of methods with fewer unknowns is the present method, SFEM, and FEM when they have equal number of nodes on the analysed plate. By studying Tables 1 and 2, one can find that the accuracy and convergence of the present method are excellent and fewer number of nodes are needed than the other two methods to yield sufficiently accurate results. The degrees of freedom required using the present method are only about 30% and 50% when compared with the four-node element and the nine-node spline element. It can be seen in Table 2 that the central deflection, the central bending moment and the corner twisting moment by the present method all converge rapidly, while the results by SFEM display a slower convergence caused mainly by the approximate elimination of the twisting curvatures at corner nodes.

Example 2 : bending of skew plate

Two types of skew plates under uniformly distributed load q shown in Fig. 2 are analysed in this paper : They are simply supported (four simply supported edges) and simply clamped (two simply supported edges and two clamped edges). Central deflections and moments of the skew plates with different skew angles are used to compare with those by the spline finite strip method (SFSM) (Tham *et al.*, 1986). The total degrees of freedom without the imposition of boundary conditions by using SFSM for plate analysis are $2NM+6N+2M+6$ under mesh $N \times M$, whereas $NM+3(N+M)+9$ is for the present

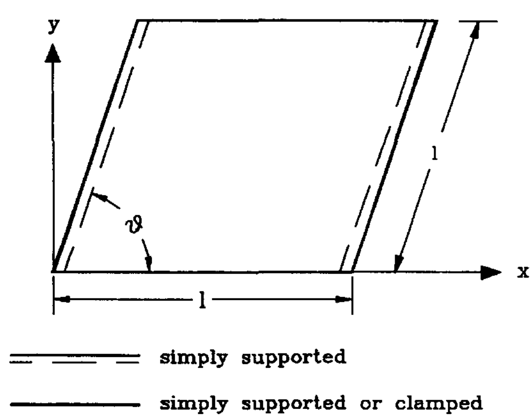

Fig. 2. Skew plate.

Table 3. Central deflections (w_c) and moments (M_x, M_y) for simply supported skew plates under uniformly distributed load

Skew angle	α		β_x		β_y	
θ	SFSM	Present	SFSM	Present	SFSM	Present
90°	0.406	0.406	0.0479	0.0479	0.0479	0.0479
75°	0.376	0.376	0.0462	0.0462	0.0476	0.0476
60°	0.294	0.293	0.0409	0.0409	0.0463	0.0463
45°	0.179	0.177	0.0318	0.0315	0.0426	0.0424
30°	0.0705	0.0688	0.0190	0.0183	0.0339	0.0334

$w_c = \alpha q L^3 L_x/(100D)$, $M_x = \beta_x q L L_x$, $M_y = \beta_y q L L_x$, $L_x = L \sin\theta$, $t = 0.1L$.

Table 4. Central deflections (w_c) and moments (M_x, M_y) for simply clamped skew plates under uniformly distributed load

Skew angle	α		β_x		β_y	
θ	SFSM	Present	SFSM	Present	SFSM	Present
90°	0.192	0.192	0.0244	0.0244	0.0333	0.0333
75°	0.176	0.176	0.0233	0.0234	0.0328	0.0329
60°	0.135	0.135	0.0203	0.0204	0.0310	0.0312
45°	0.0815	0.0814	0.0156	0.0157	0.0276	0.0278
30°	0.0327	0.0326	0.0098	0.0097	0.0216	0.0217

$w_c = \alpha q L^3 L_x/(100D)$, $M_x = \beta_x q L L_x$, $M_y = \beta_y q L L_x$, $L_x = L \sin\theta$, $t = 0.1L$.

method as mentioned above. Comparative results of two methods shown in Tables 3 and 4 are found in a very good agreement for all different skew angle cases. It should be noted that the plate meshes generated to gain the results in Tables 3 and 4 are 17×11 by SFSM and 16×16 by the present method. The number of total parameters in the present method is about 70% of those in SFSM.

Example 3 : flexural free vibration of trapezoidal plate

A simply supported trapezoidal plate is shown in Fig. 3 and it will become a rectangular plate when $b/a = 1.0$. The nondimensionalized frequency parameters of the first six modes are given in Tables 5 and 6 for the rectangular and the trapezoidal plates, respectively. An

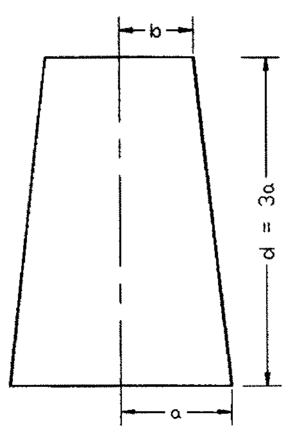

Fig. 3. Trapezoidal plate.

Table 5. Frequency parameters $\lambda = \omega(d^2/\pi^2)(\rho t/D)^{1/2}$ of simply supported rectangular plate ($b/a = 1.0$)

Mode	1	2	3	4	5	6
FEM-1	3.2505	6.253	10.029	11.279	13.033	18.070
Present	3.2502	6.2524	10.014	11.277	13.018	18.047
Exact	3.25	6.25	10.0	11.25	13.0	18.0

Table 6. Frequency parameters $\lambda = \omega(d^2/\pi^2)(\rho t/D)^{1/2}$ of simply supported trapezoidal plate ($b/a = 0.4$)

Mode	1	2	3	4	5	6
FEM-1	5.3927	9.438	14.744	15.964	21.911	23.250
FEM-2	5.4616	9.463	14.753	16.146	21.968	23.267
Present	5.3906	9.4311	14.727	15.936	21.909	23.205
Series solution	5.3896	9.424	14.685	15.911	21.700	23.146

exact theoretical solution for the natural frequencies and normal modes of the simply supported trapezoidal plate is available only for the rectangular case, when $b/a = 1.0$ (Leissa, 1969). For the cases of $b/a \neq 1.0$, Chopra and Durvasula (1971) presented an approximate solution of the problem based on trigonometric series expansion with coefficients determined by the Galerkin method and their results are generally used as a reference. Exact results for the rectangular case and series solution for the trapezoidal case are included in Tables 5 and 6. Orris and Petyt (1973) used two types of high precision, conforming, plate bending elements, one a qudrilateral (16 DOF) and the other a triangular (12 DOF), to investigate the free vibration characteristics of the same plates. For comparison, their FEM results are also quoted in Tables 5 and 6, where the frequency parameters of FEM-1 and FEM-2 were computed by using 12 quadrilateral elements with 95 total DOF and 12 quadrilateral plus 2 triangular elements with 101 total DOF, respectively, on a half plate.

The results obtained from the present method using 3×8 mesh with 66 total DOF are shown in the same tables along with the results mentioned above. Excellent agreements with the analytical solutions and better accuracy by fewer unknowns than the conforming quadrilateral and triangular elements can again be observed. The modes shapes and corresponding frequency parameters obtained from the first six modes for both rectangular and trapezoidal cases are exhibited in Fig. 4. They are similar to the nodal patterns presented by Chopra and Durvasula (1971), and Orris and Petyt (1973).

Example 4 : bending of irregular quadrilateral plate

An irregular quadrilateral plate with the coordinates of four corner nodes 1, 2, 3 and 4 is shown in Fig. 5. The central lines AB and EF connect the midpoints at two opposite sides. Midpoint C of the plate is the intersection of the central lines AB and EF. Bending analysis of this plate with two opposite sides simply supported and other two opposite sides clamped has been carried out. The results of deflection and moments at midpoint C for this plate under uniformly distributed load are given in Table 7, and deflected curves along the

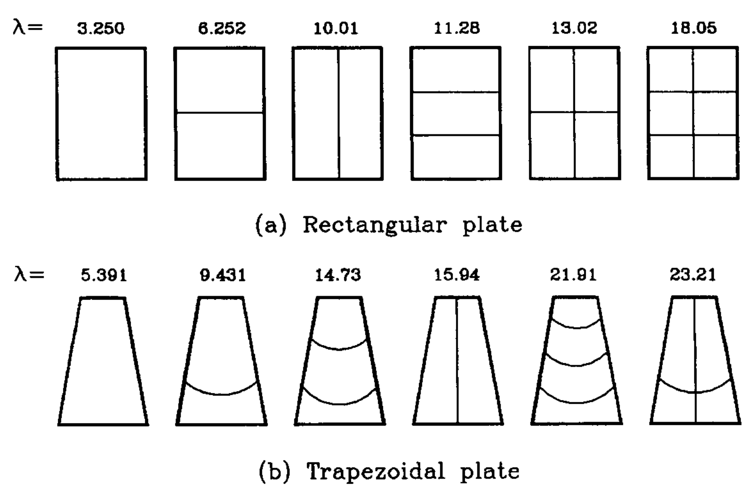

Fig. 4. Nodal patterns and frequency parameters for first six modes of simply supported rectangular and trapezoidal plates.

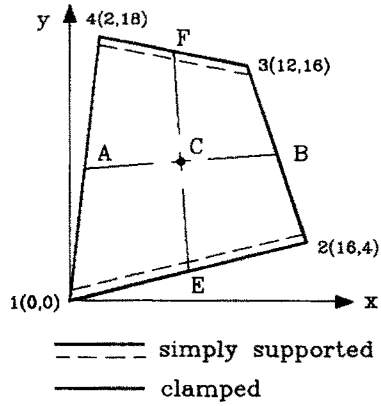

Fig. 5. Irregular quadrilateral plate.

Table 7. Deflection and moments at midpoint C for irregular quadrilateral plate under uniformly distributed load ($q = 1$, $D = 1$)

Mesh	Deflection	Bending moment M_x	Bending moment M_y	Twisting moment M_{xy}
8×8	58.885	6.082	3.717	0.2150
12×12	58.920	6.010	3.705	0.2089
16×16	58.929	5.984	3.700	0.2070

central lines AB and EF under uniformly distributed load and a concentrated force at midpoint C, respectively, are plotted in Figs 6 and 7. No comparison can be made for this example because no results for such an irregular quadrilateral plate are available in the literature. The results obtained here can serve as a test case for future researchers.

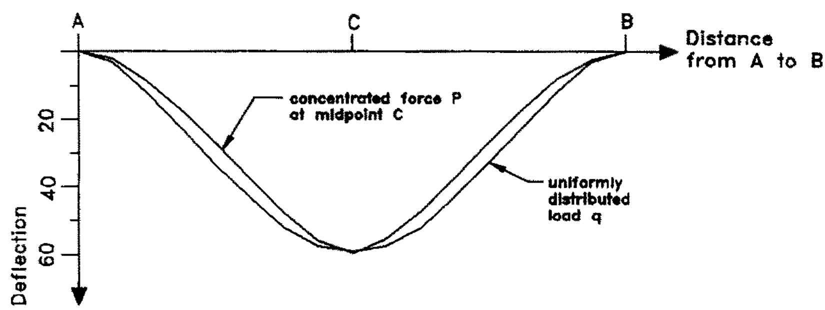

Fig. 6. Deflected curves along central line AB ($q = 1$, $P = 50$, $D = 1$, mesh 16 × 16).

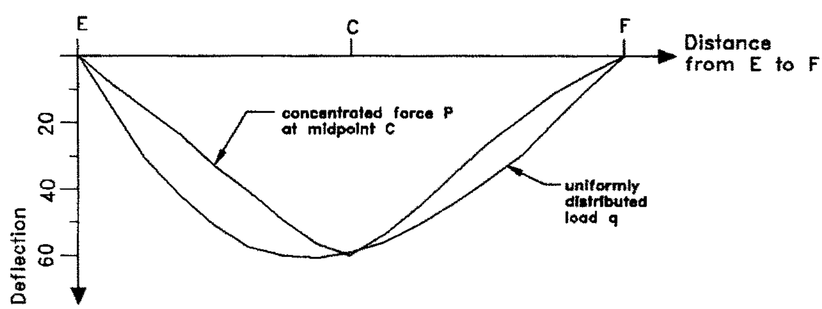

Fig. 7. Deflected curves along central line EF ($q = 1$, $P = 50$, $D = 1$, mesh 16 × 16).

CONCLUSIONS

B_3-spline functions for the interpolation of displacement in two directions are employed herein to analyse the arbitrary quadrilateral plate problems in this paper. From the theoretical considerations and the numerical examples, the present method can be summarized to achieve the following three advantages for this class of plate problems, as compared with other numerical methods.

1. By using the efficient and flexible B_3-spline functions in the displacement field, the present method does not require any discretization, thus the solutions obtained can be found to be more reliable. This method has also demonstrated with more rapid convergence and better accuracy than those discretization methods.
2. Under the mesh of $N \times M$ for an arbitrary quadrilateral plate, the present method with $(N+3)(M+3)$ parameters for the interpolation of displacement requires fewer degrees of freedom and yields more accurate results than other numerical methods, such as the conventional four-node element with $3(N+1)(M+1)$ parameters, the nine-node spline element with $2(N+1)(M+1)+(N+M+2)/2$ parameters, and the spline finite strip method with $2(N+1)(M+3)$ parameters.
3. Unlike other discretization methods, the present method does not require mesh generation so that only minimal input data is needed. Also this method avoids the additional moment modifications due to the different moment values at the sharing nodes in discretization methods.

REFERENCES

Cheung, Y. K., Fan, S. C. and Wu, C. Q. (1982). Spline finite strip in structural analysis. *Proc. Int. Conf. of Finite Element Method*, pp. 704–709, Shanghai.

Chopra, I. and Durvasula, S. (1971). Vibration of simply-supported trapezoidal plates. *J. Sound Vibr.* **19**, 379–392.

Cook, R. D., Malkas, D. S. and Plesha, M. E. (1989). *Concepts and Applications of Finite Element Analysis*. 3rd Edn. Wiley, New York.

Fan, S. C. and Luah, M. H. (1992). New spline finite element for plate bending. *J. Engng Mech. ASCE* **118**(6), 1065–1082.

Leissa, A. W. (1969). *Vibration of Plates*. National Aeronautics and Space Administration, NASA SP-160.

Leung, A. Y. T. and Au, F. T. K. (1990). Spline finite elements for beam and plate. *Comput. Struct.* **37**(5), 717–729.

Li, W. Y., Cheung, Y. K. and Tham, L. G. (1986). Spline finite strip analysis of general plates. *J. Engng Mech. ASCE* **112**(1), 43–54.

Orris, R. M. and Petyt, M. (1973). A finite element study of the vibration of trapezoidal plates. *J. Sound Vibr.* **27**(3), 325–344.

Prenter, P. M. (1975). *Splines and Variational Methods*. Wiley, New York.

Qin, R. (1982). Fundamentals and applications of spline finite-point method. *Proc. Int. Conf. on Finite Element Method*, pp. 774–780, Shanghai.

Qin, R. (1985). *Spline Function Methods of Structural Analysis* (in Chinese). People's Press of Guangxi.

Tham, L. G., Li, W. Y., Cheung, Y. K. and Chen, M. J. (1986). Bending of skew plates by spline-finite-strip method. *Comput. Struct.* **22**(1), 31–38.

Timoshenko, S. P. and Woinowsky-Krieger, S. (1959). *Theory of Plates and Shells*. 2nd Edn. McGraw-Hill, New York.

Zienkiewicz, O. C. (1977). *The Finite Element Method*. 3rd Edn. McGraw-Hill, London.